J. Synchrotron Rad. (1999). **6**, 489–491

A quantitative *in situ* Fe *K*-XAFS study ($T > 1270$ K) on the oxidation degree of iron in $(Mg_{1-x}Fe_x)_{1-\delta}O$

Nicole Hilbrandt* and Manfred Martin

Darmstadt University of Technology, Institute of Physical Chemistry, Petersenstr. 20, 64287 Darmstadt, Germany, Email:nicole@tutor.oc.chemie.tu-darmstadt.de

The point defect structure of a doped oxide, $(Mg_{1-x}Fe_x)_{1-\delta}O$, was quantitatively determined by *in situ* high temperature X-ray absorption spectroscopy (1270 K<T<1470 K). Spectra were recorded under defined oxygen activity at the dopant's K-edge. The degree of oxidation α versus T, a_{O_2} and x can be consistently described by a simple defect model. This model considers divalent iron ions ($R_{Fe\text{-}O}$=215.8 pm), randomly dissolved in the cation sublattice, and a defect associate between two trivalent iron ions and a cation vacancy ($R_{Fe\text{-}O}$=205.0 pm). Indications of trivalent ions occupying interstitial sublattice sites were found near the $(Mg_{1-x}Fe_x)_{1-\delta}O/MgFe_2O_4$ phase boundary.

Keywords: *in situ* X-ray absorption spectroscopy; point defect structure; defect association; degree of oxidation of iron

1. Introduction

Iron-doped magnesium oxide, $(Mg_{1-x}Fe_x)_{1-\delta}O$, is one of the main compounds of the Earth's lower mantle. The mixed oxide determines the Earth's mantle's chemical and physical properties via the oxidation degree of iron and related point defects under high pressure, p, and at high temperature, T (McCammon, 1997; Peyronneau & Poirier, 1989; Poirier *et al.*, J.P., 1996). In the past, various techniques have been applied to characterize its defect-related properties using most of the time quenched specimens. Nowadays, *in situ* techniques, such as thermopower or conductivity measurements (Peyronneau & Poirier, 1989; Poirier *et al.*, J.P., 1996; Wood & Nell, 1991) and *in situ* Mossbauer spectroscopy (Becker & Dreher, 1989) have gained prominence. However, although the system is widely studied, there is still a lack of direct (non-modelled) information on the valence and details of the local environment of the dopant. To study these properties as function of temperature, T, oxygen activity, a_{O_2}, and composition, x, we have performed the first systematic *in situ* XAFS-measurements on $(Mg_{1-x}Fe_x)_{1-\delta}O$ (for details: Hilbrandt & Martin, 1998).

2. Experimental

The doped polycrystals of $(Mg_{1-x}Fe_x)_{1-\delta}O$ were prepared by mixing, ball milling and isostatically compressing (p=14 MPa) appropriate amounts of MgO (J. Matthey, 99.99%, ultrapur) and hematite, Fe_2O_3, (Ventron, >99%) powders. The compacts were equilibrated for 4-6 days at 1573 K ($a_{O_2}=10^{-8.3}$) within the stability field of the iron-doped MgO (Hilbrandt & Martin, 1998). The phase purity was monitored by Mossbauer spectroscopy, X-ray diffraction or SEM-WDX analysis. The composition x and chemical purity of the specimens were determined by electron microprobe analysis and EDS. The samples were homogeneous within $\Delta x \leq \pm 0.002$ and above the resolution limit of EDS (Δx= ±0.01-0.001) any impurities were detected. For the *in situ* XAFS experiments, the sintered specimens were polished down to a thickness of 77-165 ± 1 μm (μd<2.6, $\Delta\mu d \leq 1.6$). To ensure that the absorber contained neither pinholes nor cracks, the samples were light-tested prior to the experiments.

The X-ray absorption studies were carried out in a high temperature furnace (T_{max} ≈1500 K) under continuous gas flow. Either CO/CO_2 or N_2/air gas mixtures were used to establish conditions within the single-phase field of $(Mg_{1-x}Fe_x)_{1-\delta}O$ (Hilbrandt & Martin, 1998). The experimental set-up was installed in HASYLAB' s bending magnet beamline X 1.1 at DESY (E=4.45 GeV; I=60-100 mA). To reject higher harmonics, the double-crystal *Si*(111)-monochromator was detuned and stabilized to 50% of the incident intensity, I_0, at the absorption edge. The energy was calibrated to the K-edge position, E_0, of a simultaneously measured Fe reference (Goodfellow, 99,85%, light-tested, 8 μm thick) assigning E_0=7.1112 keV (Bearden & Burr, 1967). Ionisation chambers filled with N_2 were used to detect the photon intensities. Data reduction and analysis were performed using the software package WinXAS (Ressler, 1997). In particular, the cumulant expansion formalism was applied (Koningsberger, 1988). To identify the site preference of iron, multiple scattering cluster calculations within the correlated Debye model (Sevillano *et al.*, 1979) were performed on the Fe-K EXAFS of iron in MgO (MgO - space group Fm3m, a=421.12 pm, Θ_D=743 K (Landolt-Börnstein, 1979)) using the FORTRAN77 code FEFF6.01 (Zabinsky *et al.*, 1995). In addition, the calculated spectra were used as theoretical standards to characterize the EXAFS of Fe^{2+} in $(Mg_{0.894}Fe_{0.106})_{1-\delta}O$ measured at low a_{O_2} and 1270 K<T<1470 K in detail. Further multiple-shell data analysis was carried out using experimental phases and amplitudes extracted from these high temperature EXAFS functions (system internal standard). As the Debye-Waller factor and higher cumulants were proven to depend only on T, they were kept constant during EXAFS refinement. For further details see archive http://ixs.iit.edu/xafsx *No. 113185150.*

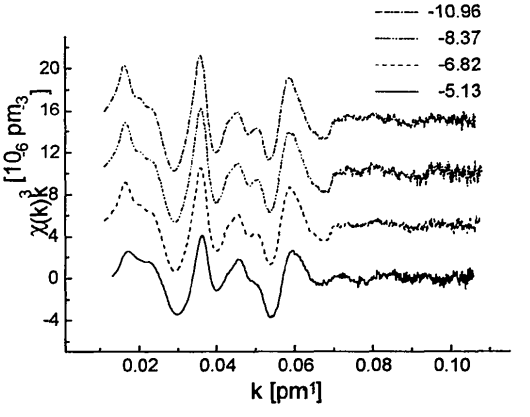

Figure 1
$(Mg_{0.894}Fe_{0.106})_{1-\delta}O$: Dependence of $\chi(k)k^3$ on the oxygen activity (see legend); T= 1468 K; Fe-K edge (k=0.01-0.11 pm^{-1}).

3. Results and Discussions

Within the following section, emphasis will be placed on results obtained for $(Mg_{1-x}Fe_x)_{1-\delta}O$ samples with x=0.106 (To judge the EXAFS data quality, see Fig. 1). The compound was systematically studied within a temperature range of T=1273 K to 1468 K under 3-6 different oxygen activities to avoid quenching effects In Fig. 2 the evolution of the Fe-K XANES spectra and the pre-edge peaks with oxygen activity (T=1468 K) are depicted. With increasing a_{O_2} ($\log a_{O_2}$ >-8.4), the whole XANES shifts about +1 eV and becomes increasingly similar to the spinel spectrum. The changes in the XANES are accompanied by a decline in the peak height of each feature in the radial structure function (Fig. 3). The first peak continuously broadens and the peak maximum advances to lower R values. X-ray absorption spectra, recorded at 1270 K and 1375 K, provide similar trends compared with Fig. 2 and 3.

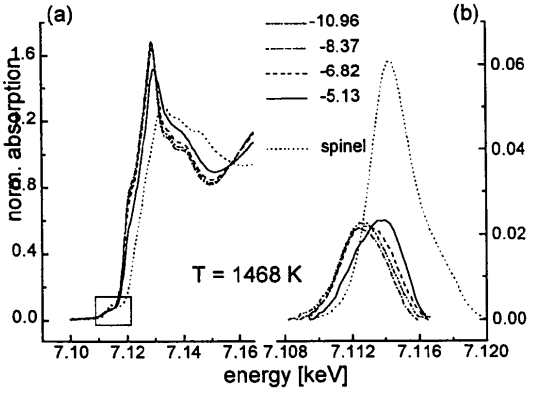

Figure 2
Evolution of (*a*) the Fe-K-XANES of $(Mg_{0.894}Fe_{0.106})_{1-\delta}O$ and (*b*) the background corrected pre-edge region as a function of oxygen activity at 1468 K. For comparison, the diagrams are complemented by the Fe-K spectrum of $MgFe_2O_4$ (finely dashed)

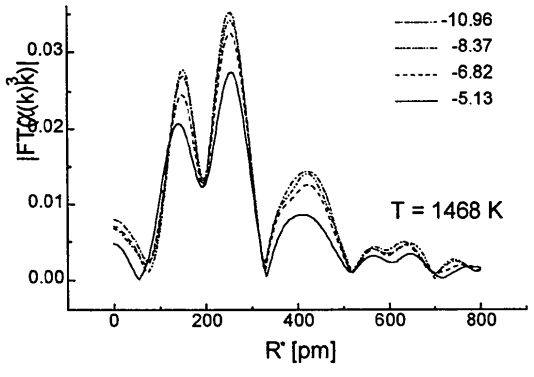

Figure 3
Dependence of the radial structure function of iron in $(Mg_{0.894}Fe_{0.106})_{1-\delta}O$ on the oxygen activity; T= 1468 K; Fourier transformation over 0.026-0.102 pm^{-1} applying a Bessel window.

To quantify the observed trends in the EXAFS in terms of iron oxidation and site distribution of iron within the MgO lattice, a combined single-shell/two-shell refinement of the first Fe-O coordination sphere between 100 and 180 pm was performed. If several iron-containing defect species contribute to the EXAFS, the results of a single shell analysis represent, to a first approximation, the averaged oxygen environment of the iron species. To prevent correlations between the EXAFS parameters by using the system internal standard (see section 2) at given temperature, a maximum of 2 shells can be refined.

Over the temperature interval from 1273 to 1468 K, the quality of the refinement is significantly improved by considering a second shell to describe the first peak of the Fourier transform. The coordination sphere can be decomposed in a Fe-O shell at $\overline{R_1}$ =205.0 pm and $\overline{R_2}$ =215.6 pm. The latter distance coincides with that of octahedrally coordinated Fe^{2+}, and based on Shannon radii (Shannon & Prewitt, 1972), the first one can be ascribed to Fe^{3+} also coordinated by six oxygen ions. This interpretation coincides with the observations in the XANES: the pre-edge peak is shifted to higher energies (oxidation) but remains weak in intensity (octahedral coordination). The degree of oxidation can be calculated by two different methods based on the EXAFS analysis. The results both coincide to within $\Delta\alpha$= 0.03:

I. As multiple-shell analysis gives effective coordination numbers, N^*, the ratio $N^*_{Fe^{3+}}/(N^*_{Fe^{2+}} + N^*_{Fe^{3+}})$ describes α. The error of this analysis, related to the error in N^*,(ΔN^*~0.2) is on the order of $\Delta\alpha$~0.04.

II. The average distance of close-lying shells, which was determined by single-shell fitting, can be described by the sum of the R_i weighted by their molar fractions. As the error in R_1 (ΔR_1~2 pm) is large compared to R_2 (ΔR_2~0.2pm), the error in α is largely determined by those in R_1 ($\Delta\alpha$~0.06).

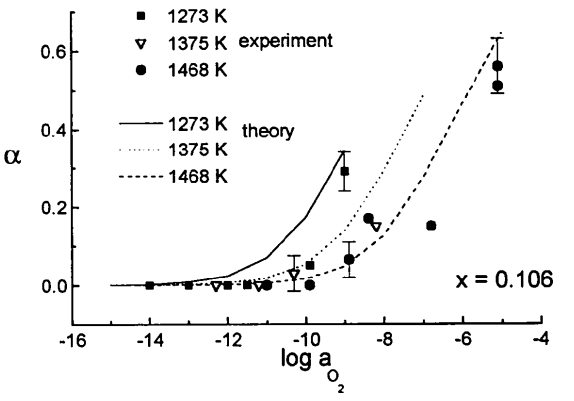

Figure 4
Degree of oxidation, α, both inferred from EXAFS analysis at different temperatures and calculated from the discussed point defect model (K_1 see Gourdin *et al.*, 1979); x=0.106.

The averaged values of α are depicted in Fig. 4. The behaviour of α as a function of T, a_{O_2} and even x (Hilbrandt & Martin, 1998) can be consistently described by a defect model based on the following oxidation equilibrium (for equilibrium constant K_1 see Gourdin *et al.*, 1979):

$$2\,Fe^x_{Mg} + \tfrac{1}{2}O_2 \;??\; \blacklozenge\; (Fe^{\cdot}_{Mg}V''_{Mg}Fe^{\cdot}_{Mg})^x + O^x_O \qquad (1)$$

Under consideration of the iron balance

$$[Fe]_{total} = x(1-\delta) = [Fe^x_{Mg}] + 2\,?[(Fe^{\cdot}_{Mg}V''_{Mg}Fe^{\cdot}_{Mg})^x] \qquad (2)$$

$$\delta = [(Fe^{\cdot}_{Mg}V''_{Mg}Fe^{\cdot}_{Mg})^x] \qquad (3)$$

the oxidation degree of iron can be calculated:

$$\alpha = 2 ? \frac{[(Fe_{Mg}^{\times} V_{Mg}'' Fe_{Mg}^{\times})^{x}]}{[Fe]_{total}} \quad (4)$$

At appropriate low oxygen activity, the XAFS was identified to belong to $Fe_{Mg}^{\times}$ FEFF simulations and comparison with XANES-standards (Hilbrandt & Martin, 1998). This opens the possibility of reconstructing the XANES of the trivalent iron species bound in $(Fe_{Mg}^{\times} V_{Mg}'' Fe_{Mg}^{\times})^{x}$ via the following equation:

$$\mu_{Fe^{3+}} = \frac{\mu - \mu_{Fe^{2+}}}{\alpha} + \mu_{Fe^{2+}} \quad (5)$$

In Fig. 5 the reconstructed near edge structures of Fe^{3+} in $(Mg_{1-x}Fe_x)_{1-\delta}O$ at T=1375 and 1468 K are depicted. The spectra show all of the characteristics of trivalent iron in octahedral coordination: With respect to the divalent species, the XANES is shifted to higher energies due to the increase in valence. The shift in the absorption maximum, ΔE_{max}= +2 eV along with the decrease in "white line" intensity and the increase of the absorption beyond E_{max} are typical for octahedrally coordinated iron (Garcia *et al.*, 1986, Waychunas *et al.*, 1983). The intensity changes can be attributed to changes in the phase functions of the absorber as demonstrated by Garcia *et al.*, 1986. Additionally, the occurrence of a pre-edge peak, weak in intensity and shifted by approx. +2 eV, is characteristic for trivalent iron on sites with O_h-symmetry (Shulman *et al.*, 1976). The consistency in reproduction can be regarded as a further proof for the validity of the proposed defect model.

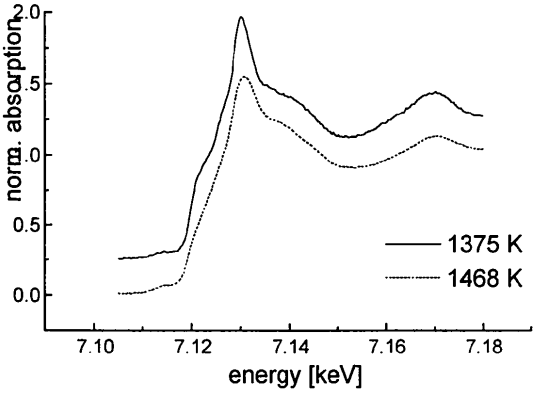

Figure 5
Reconstructed Fe-K XANES of trivalent iron bound in a trimer (T=1375 and 1468 K).

Evidence of iron partially occupying interstitial sites was also found for $(Mg_{0.894}Fe_{0.106})_{1-\delta}$. At T=1468 K and log a_{O_2} = -5.13, close to the $(Mg_{1-x}Fe_x)_{1-\delta}O/MgFe_2O_4$ phase boundary, the two-shell refinement is remarkably unstable. Without introducing constraints, Fe-O distances at R_1=192 pm and R_2=213.2 pm were obtained. The shorter Fe-O distance can be attributed to trivalent iron in tetrahedral oxygen coordination. The longer one can be interpreted as the weighed-average Fe-O distance of the iron species $Fe_{Mg}^{\times}$ and $(Fe_{Mg}^{\times} V_{Mg}'' Fe_{Mg}^{\times})^{x}$. In addition, a slight increase in intensity of the shifted pre-edge peak is observed in the XANES which is attributed to small fractions of iron within the interstitial sublattice (see above).

4. Conclusions

As a model system for non-stoichiometric doped oxide, $(Mg_{1-x}Fe_x)_{1-\delta}O$ was investigated to quantitatively describe the point defect structure by *in situ* Fe-K X-ray absorption spectroscopy. The experiments were performed under defined thermodynamic conditions; i.e. at high temperature (T=1273-1468 K) and under fixed oxygen activity within the stability field of the mixed oxide. To characterize the defect structure, the nearest neighbour Fe-O bond lengths and coordination numbers for x=0.106 were analysed to determine of the oxidation degree of the dopant. The Fe-K EXAFS predominately consisted of two octahedrally coordinated iron species. These were identified by their bond lengths: Fe^{2+} (R=215.8 pm) and Fe^{3+} (R=205.0 pm), both occupying magnesium lattice sites. The observed dependence of α with T and a_{O_2} can be described by a defect model which considers Fe^{2+} randomly to be distributed within the cation sublattice and Fe^{3+} to be bound in a defect associate between two Fe^{3+} and a cation vacancy. As the XANES of Fe^{2+} in $(Mg_{0.894}Fe_{0.106})_{1-\delta}O$ was available at low oxygen activity, the XANES of Fe^{3+} bond in the defect associate could be reconstructed. Additionally, indications for Fe^{3+} in the interstitial sublattice were found at high a_{O_2}.

We would like to thank H. Teuber for assistance during measurements on beamline ROEMOII, HASYLAB (DESY). N.H. gratefully acknowledges the fellowships by the Friedrich-Ebert and the Alexander-von-Humboldt Foundation. The Deutsche Forschungsgemeinschaft financially supported these investigations.

References

Bearden, J.A. & Burr, A.F. (1967). *Rev. Mod. Phys.* **39,** 125.
Becker, K.D., Dreher, S. (1989). *Ber. Bunsen Ges. Phys. Chem.* **93**(11), 1382.
Garcia, J., Bianconi, A., Benfetto, M. & Natoli, C.R. (1986). *J. Phys. Colloq. C8, Suppl.* **12**(47), 49.
Gourdin, W.H., Kingery, W.D. & Driear, J. (1979). *J. Mater. Soc.* **14,** 2074.
Hilbrandt, N. & Martin, M. (1998). *Ber. Bunsen Ges. Phys. Chem.* 12, 1747.
Koningsberger, D.C. & Prins, R. (Ed.): X-ray absorption: Principles, applications, techniques of EXAFS, SEXAFS and XANES, *Chemical Analysis* **92,** Wiley & Sons (1988).
Landolt-Börnstein, *Zahlenwerte und Funktionen aus Naturwissenschaft und Technik,*,Springer, Berlin (1979).
McCammon, C. (1997). *Nature* **387**(6634), 694.
Peyronneau, J. & Poirier, J.P. (1989). *Nature* **342,** 537.
Poirier, J.P., Goddat, A. & Peyronneau, J. (1996). *Philos. Trans. R. Soc. Lond. Ser. A Math. Phys. Eng. Sci.* **354**(1711), 1361.
Ressler, Th. J. (1997). *Phys. IV France, Suppl.* **7,** C2-269.
Sevillano, E., Meuth, H. & Rehr, J.J. (1979). *Phys. Rev. B* **20**(12), 4908.
Shannon, R.D. & Prewitt, C.T. (1969). *Acta Crystallogr.* **B25,** 925.
Shulman, G.R., Yafet, Y., Eisenberger, P. & Blumberg, W.E. (1976). *Proc. Natl. Acad. Sci. USA* **73**(5), 1384.
Waychunas, G.A., Apted, M.J. & Brown, G.E.. (1983). *Phys. Chem. Minerals* **10,** 1.
Wood, B.J., Nell, J. (1991). *Nature* **351**(6324), 309.
Zabinsky, S.I., Rehr, J.J., Ankudinov, A., Albers, R.C. & Eller, M.J.(1995). *Phys. Rev. B* **52**(4), 2995.

(Received 10 August 1998; accepted 28 January 1999)